



Evaluation of the interlayer interactions of few layers of graphene

Junto Tsurumi, Yuika Saito*, Prabhat Verma

Department of Applied Physics, Osaka University, 2-1 Yamadaoka, Suita, 565-0871 Osaka, Japan

ARTICLE INFO

Article history:

Received 24 August 2012

In final form 6 December 2012

Available online 19 December 2012

ABSTRACT

We examined the number of layers in graphene using Raman microscopy and investigated the interlayer interactions by understanding the layer stacking through the $E^*(\text{low})$ mode measured in Raman spectroscopy designed for low-frequency observation. The number of layers in Raman image was determined from the $G/2D$ intensity ratio, and the interlayer stacking for 2, 3 and 4 layers was understood from the positions of the $E^*(\text{low})$ mode. While most part of sample showed AB stacking, a small area showed random stacking of layers. Low-frequency Raman spectroscopy revealed that such sample area was consisted of weakly interacted random stacking of graphene layers.

© 2012 Elsevier B.V. All rights reserved.

1. Introduction

Graphene, with high carrier mobility, has attracted remarkable interest for its application in semiconductor devices ever since Novoselov and Geim successfully demonstrated the mechanical exfoliation method in 2004 for producing single and multilayer graphene [1]. The carrier mobility of graphene has been reported to be as high as $200,000 \text{ cm}^2/\text{Vs}$ [2,3], which is about 100 times higher than that of silicon. Therefore, graphene has an excellent potential to be utilized in high-speed semiconductor devices. However, since graphene does not have a natural band gap, one needs to artificially create a band gap for its actual application in transistors and other devices [4,5]. The width of such a band gap for graphene samples containing a few layers depends on the interlayer interaction and it can be adjusted by the strength of applied electric field [6,7].

With the growing interest in graphene-based technologies, there exist several established methods to produce excellent quality graphene with single to multilayered structures, such as mechanical exfoliation [1,8], thermal expansion [9], surface segregation [10] epitaxial growth [11] and chemical vapor deposition [12]. These methods produce good samples, suitable especially for the investigation of physical properties [13] and industrial applications, which requires large sample area [14]. One of the interesting points about these growth techniques is that graphene samples made by different methods may exhibit different interlayer interactions. For example, graphene prepared by alcohol chemical vapor deposition has a weaker interlayer interaction than the mechanically exfoliated graphene [12], because the former has slightly twisted stacking of layers. Since the carrier mobility

strongly depends on the interlayer interaction, it is essential to investigate the stacking of the layers to understand the interlayer interaction for future device applications. There are several reports that investigated interlayer interactions by monitoring the second-order of the defect band (2D-band) in Raman spectra measured from graphene samples [15,16]. The band structure of graphene depends on the interlayer interaction, which affects the shape of the 2D-band in Raman spectra. For example, a weaker interaction caused by the twisted stacking narrows the spectral width of 2D-band [12]. Likewise, when the interlayer stacking of a multilayer graphene is random, the integrated intensity of 2D-band increases due to the weakened interlayer interaction to resemble non-interacting single layers that have stronger 2D-bands [17]. The intensity ratio between the graphite-like vibrational band of graphene (G-band) and the 2D-band, *i.e.*, I_G/I_{2D} , (the $G/2D$ intensity ratio) for such samples may become as low as that of single layer graphene [14] due to the weak interlayer interactions in random stacking. On the other hand, low-frequency Raman spectroscopy is a direct way to investigate the interlayer bonding. The $E^*(\text{low})$ mode is one of the low-frequency modes that can be observed in a Raman spectrum of multi layer graphene [18–20]. It arises from the relative vibrations of the neighboring layers, hence the strength of interlayer bonding is reflected in the frequency of the $E^*(\text{low})$ mode [21]. The $E^*(\text{low})$ phonon frequency can indeed be a probe for interlayer potential energies [22]. However, there are only limited reports on the experimental measurements of the $E^*(\text{low})$ mode for graphite [23,24], because this mode appears reasonably close to the Rayleigh line and hence it is technically difficult to distinctly separate out this Raman mode from the strong Rayleigh background in the experimental measurements. Specific adjustments in the experimental setup are required to selectively reject the Rayleigh background. Only a recent work has experimentally investigated the dependence of $E^*(\text{low})$ mode on the number of layers [25].

* Corresponding author. Fax: +81 6 6879 4711.

E-mail address: yuika@ap.eng.osaka-u.ac.jp (Y. Saito).

Here in this report, we investigated the interlayer interaction to understand the stacking for 2, 3, and 4 layer graphene samples by exploring the low-frequency $E^*(\text{low})$ mode in Raman scattering. Our experimental setup was specifically modified for the observation of low-frequency Raman modes, where we could effectively reject the Rayleigh background. In our experiments, we prepared graphene samples with different number of layers and performed micro Raman imaging on our samples to determine the number of layers through the $G/2D$ intensity ratio. After determining the number of layers, we measured the $E^*(\text{low})$ mode for 2, 3, and 4 layers of graphene. In addition, we measured the $E^*(\text{low})$ mode for a graphite sample for comparison and calibration. The inter-layer interactions in our graphene samples were explored through the low-frequency Raman spectroscopic analysis.

2. Methods and materials

Graphene samples for present Letter were prepared by mechanical exfoliation method from a piece of highly ordered pyrolytic graphite (HOPG). A glass substrate, on which the graphene samples were prepared, was cleaned with ethanol in an ultrasonic bath and was then treated with compound liquid of hydrochloric acid and hydrogen peroxide. Exfoliated graphene extracted on a scotch tape was transferred to the clean substrate. The sample was washed with acetone to remove the residual paste of the scotch tape. The lattice structure of HOPG largely consists of closest-packed stacking of graphene sub-lattice with either AB type stacking (about 85%) or ABC type stacking (about 15%) [26].

Raman measurements for both spectroscopic analysis and microscopic imaging of graphene samples were performed with an incident laser of wavelength 532 nm, which was focused on the sample through an oil immersion objective lens that had a numerical aperture 1.4 and magnification 60. The Raman scattered signal was collected through the same objective lens, and was guided through a 40 μm slit to a spectrometer equipped with a charge-coupled device camera. The typical laser powers used for the high-frequency and the low-frequency Raman scattering measurements were 3 and 15 mW, respectively. Raman spectra in both high-frequency and low-frequency regions were measured with the same optical system, but with different Rayleigh rejection optics. For measurements below 100 cm^{-1} , Raman scattered signal of the sample was separated from the backscattered Rayleigh signal by using a filter called Braggrate notch filter, which was purchased from OptiGrate. This filter can separate the Raman shift of $\sim 10 \text{ cm}^{-1}$ from 532 nm excitation line. Two similar filters were inserted at an opposite dihedral angle to compensate the optical path. During the imaging experiments, the sample was fixed on a piezo-controlled stage, which was moved at the steps of 222 nm, a value that corresponds to the diffraction limit of the excitation laser wavelength.

3. Results and discussions

3.1. Determination of the layer numbers by micro Raman imaging

In the first part of the experiments, we recorded an optical image of the exfoliated graphene sample, which is shown in Figure 1a. A slight variation of contrast in optical image qualitatively indicates variation in number of graphene layers. However, a quantitative estimation of number of layers in optical image is not possible without a spectroscopic analysis. We then measured Raman spectra from the same area of the sample in the spectral range of 1200–3000 cm^{-1} , where the integrated intensities of the G-band and the 2D-band were estimated after proper normalization. The number of graphene layers in the sample was estimated through the

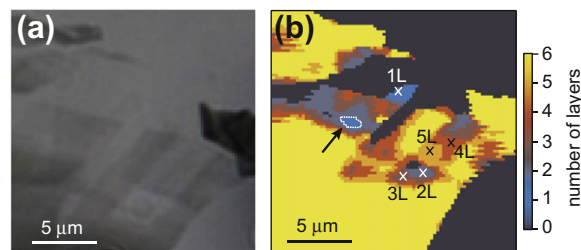


Figure 1. (a) Optical transmission image of graphene sample fixed on a glass substrate. Slight variation in contrast indicates variation in the number of graphene layers in the sample. (b) Raman image mapping the number of graphene layers in the same area of the sample. The colors indicate the number of layers estimated from the $G/2D$ intensity ratio in Raman spectra. The area marked by an arrow and enclosed by white dotted line consists of random stacking layers. The cross marks indicate the points from where low-frequency Raman scattering was measured.

$G/2D$ intensity ratio and was mapped to construct a Raman image of layer distribution in the sample, which is shown in Figure 1b. The colors in Figure 1b correspond to the $G/2D$ intensity ratio, from which the variation of number of layers in different parts of the sample could be realized, as also indicated in the figure. If one looks into the literature, the absolute value of $G/2D$ intensity ratio for a particular number of layers differs from one report to other [27,28]. Therefore, we made a histogram of $G/2D$ intensity ratio from the Raman spectral mapping and determined the ratio that corresponds better to our experimental system. In this way, we could assign the number of layers from 1 to 5 across the sample with a diffraction limited spatial resolution. We also located an area indicated by an arrow and shown by white dotted enclosure in Figure 1b where it was difficult to assign the number of layers, because the spectral behavior of this part of the sample was ambiguous. While extraordinarily higher intensity of the 2D-band gave a low value of the $G/2D$ intensity ratio that resembles the intensity ratio for a single layer, the entire spectral shape was different from that of a single layer graphene.

Figure 2 shows high-frequency Raman spectra measured from the sample locations denoted by cross marks in Figure 1b, indicating different number of layers. In addition, Raman spectra were also measured from the area enclosed by the white dotted line that showed ambiguous behavior, and from a graphite sample.

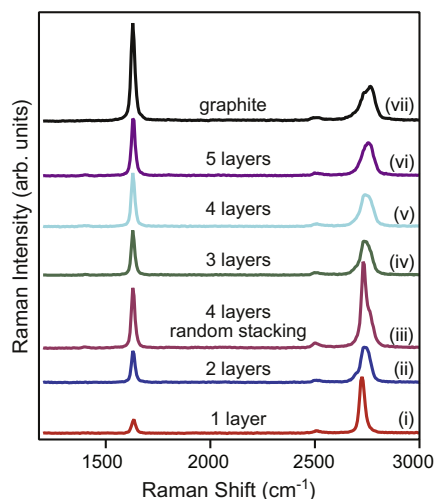


Figure 2. High-frequency Raman spectra of 1–5 layers of graphene, measured at the cross marks shown in Figure 1b. Raman spectrum from the area enclosed by white dotted line in Figure 1b is shown by (iii), and Raman spectrum from a graphite sample is shown by (vii).

Spectrum (iii) in Figure 2 was taken from the area within white dotted line, while spectrum (vii) represents the graphite sample. As the figure shows, the intensity of G-band is roughly proportional to the number of graphene layers. While we utilized the G/2D intensity ratio to estimate the number of layers in Raman image, the spectral shape of 2D-band can also be utilized to estimate the number of layers. The number of layers estimated from these methods, namely from the G/2D intensity ratio and the spectral shape of the 2D-band, give the same result for all spectra from (i) to (vi), except for the spectrum (iii). While the spectral shape of the 2D-band and the normalized intensity of the G-band in spectrum (iii) suggest the presence of 4 layers, the value of the G/2D intensity ratio is similar to that of a single layer. The two results together suggest that this area of the sample may contain 4 layers of graphene, which are randomly stacked, so that their interlayer interaction is weak enough to make them behave like weakly interacting independent layers. Indeed, some researchers have also suggested that the extraordinary high intensity of the 2D-band is an indication of random stacking of several graphene layers [12,17]. We therefore conclude that the area surrounded by white dotted line in Figure 1b contains randomly stacked 4 layers of graphene, which we would discuss in more details. We speculate that the local random stacking of graphene layers in our sample was a result of uncontrolled inhomogeneous stress between the scotch tape and the glass substrate, which might have occurred during the transferring of graphene layers from the scotch tape to the glass substrate. This uncontrolled stress might have misaligned the layers locally.

3.2. Investigation of the layer stacking by low-frequency Raman spectroscopy

Further, we measured low-frequency Raman spectra from the same locations of the sample as before, which are presented after background correction in Figure 3. Since low-frequency Raman

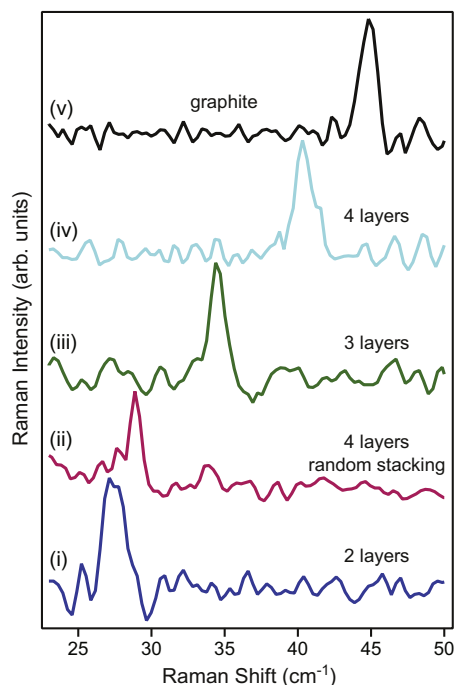


Figure 3. Low-frequency Raman spectra of 2, 3, and 4 layers of graphene, measured at the cross marks shown in Figure 1b. Raman spectra from the area enclosed by white dotted line in Figure 1b and from a graphite sample are shown by (ii) and (v), respectively.

modes do not exist for single layer, it is not included in the figure. Also, the spectrum for 5 layers of graphene was similar to that of graphite, hence it is also excluded in Figure 3. The peak observed at 44 cm^{-1} in Raman spectrum of graphite can be assigned to the $E^*(\text{low})$ mode, which is one of the low-frequency Raman modes present in graphite [23]. Depending upon the number of layers, the peak position of this mode varies within the range of $30\text{--}40\text{ cm}^{-1}$ in graphene samples. As shown in Figure 3, the peak positions of the $E^*(\text{low})$ mode for graphene samples with 2, 3, and 4 layers in our experiments were found at 27, 36 and 40 cm^{-1} , respectively, which agree well with the calculated and experimental peak positions of the same number of layers in closest-packed graphene samples reported earlier [19,21,25]. In Ref. [25], which is the only experimental work on low frequency Raman spectroscopy of graphene reported so far in our knowledge, the samples were measured in cross polarized configuration, which means the authors selectively measured only the off diagonal tensor component. However, in the present Letter, we have measured both diagonal and off diagonal components with high-NA objective lens without polarization selection. The slight difference in Raman shift frequency can be attribute to the difference of the substrate.

The increase in Raman frequency of the $E^*(\text{low})$ mode with increasing number of layers can be explained by the suppression of the vibration by the interference of the neighboring layers.

We also measured the low-frequency Raman spectrum of the sample area containing random stacking of graphene layers enclosed by the white dotted line in Figure 1b, which is presented by spectrum (ii) in Figure 3. The $E^*(\text{low})$ mode in this spectrum appears at 29 cm^{-1} . The value of this peak position is quite similar to that for the sample area containing 2 layers of graphene. As we noted earlier from the high-frequency Raman measurement, the intensity of the G-mode and the shape of the 2D-mode measured from this area of the sample indicated the presence of 4 layers of graphene, while the intensity of the 2D-mode confirmed weak interlayer interactions or the random stacking of the graphene layers. By combining the layer information obtained from the high-frequency and the low-frequency Raman measurements, we propose that the area enclosed by the white dotted line in Figure 1b contains either a pair of 2 layers, which have closet-packed stacking (2 + 2 layers), or 2 layers in closet-packed stacking plus two single layers of graphene (2 + 1 + 1 layers). An extra upshift of about 2 cm^{-1} in the peak position of $E^*(\text{low})$ mode coming from this part of the sample in comparison with that of a 2 layer graphene could be explained by the weak interlayer interaction that exists even when the stacking is random. This weak interlayer interaction, which is not completely ignorable, is responsible for a slight increase in the phonon frequency of the low-energy Raman mode. The interlayer interaction energy for the randomly stacked area was estimated to be $11.3 \times 10^{18}\text{ Nm}^{-3}$ from the peak position of the low frequency Raman mode [25]. This value is weaker than that for the closed packed 4 layers, which is estimated to be $12.6 \times 10^{18}\text{ Nm}^{-3}$, due to the mismatch between the two sets of bilayers.

Thus, by analyzing the low-frequency Raman scattering of graphene sample, we are able to understand the interlayer interactions for complicated or randomly stacked multilayered graphene.

The random stacking structure can be modeled as the overlap of two graphene layers that are twisted with respect to one another. There have been some recent reports on the twisted bilayer graphene studied by high frequency Raman spectroscopy [29,30], where the G-band intensity was found to dramatically enhance around the twist angle of 10 degrees. The 2D band showed irregular shapes between the twist angles of 0–20 degrees and the intensity of 2D band appeared to be larger than that of single layer when the twist angle was larger than 15 degrees. Considering these reports, our results suggest that the twist angle in our case was less than 10

degrees because the intensity of G-band is not as high as that at the resonance angle and the intensity of 2D band is similar to that of a single layer. However, it is difficult to establish a relationship between the low frequency Raman mode and the twist angle at this point.

Here we would like to note that the Raman frequency of the E* (low) mode can have an additional shift due to a possible interaction of the graphene layer with the glass substrate. If the sample is multilayered, the Raman frequency of upper layers of graphene would be influenced only by the interaction with the neighboring lower graphene layer, while the bottom layer of graphene would be influenced by the interactions with both the neighboring upper graphene layer and the glass substrate. Therefore, the spectrum of a multilayer sample may contain inhomogeneous broadenings of Raman peaks coming from slight difference in interactions for different layers of the sample.

4. Conclusions

In conclusion, we have estimated the interlayer interaction of a graphene sample containing different number of layers by low-frequency Raman spectroscopy. While commonly used high-frequency Raman spectroscopy can be used to estimate the number of layers, it sometimes gives incorrect information, particularly when Raman scattering shows ambiguous behavior due to random stacking of the layers. Low-frequency Raman spectroscopy, on the other hand, gives direct information about the interlayer interaction, and hence can be used for a precise estimation of both, the number of layers and the interlayer interaction or the stacking behavior of the layers. Raman imaging provides important information about the existence of the disordered layers within the closest-packed area. We identified an area in our sample where Raman scattering showed ambiguous behavior, and analyzed this area with low-frequency Raman spectroscopy. We could conclude that this area consisted of 4 graphene layers, which were stacked either in the form of two pairs of closet-packed stacking, or in the form of 2 layers in closet-packed stacking plus two single layers. Such information cannot be extracted from the commonly used high-frequency Raman spectroscopy. Low frequency Raman spectroscopy combined with imaging technique helped in reveal-

ing the stacking structure and the interlayer interactions in multilayered graphene system, which could be essential for the investigation of the spatial variation in the band-gap energy for future device applications.

Acknowledgement

This work was supported by JSPS Asian CORE Program.

References

- [1] K.S. Novoselov et al., *Science* 306 (2004) 666.
- [2] A.K. Geim, K.S. Novoselov, *Nat. Mater.* 6 (2007) 183.
- [3] K.I. Bolotin et al., *Solid State Commun.* 146 (2008) 351.
- [4] P.R. Wallace, *Phys. Rev.* 71 (1947) 622.
- [5] B. Partoens, F.M. Peeters, *Phys. Rev. B* 74 (2006) 075404.
- [6] T. Ohta, A. Bostwick, T. Seyller, K. Horn, E. Rotenberg, *Science* 18 (2006) 5789.
- [7] Y. Guo, W. Guo, C. Chen, *Appl. Phys. Lett.* 92 (2008) 243101.
- [8] A.K. Geim, *Science* 324 (2009) 1530.
- [9] M.J. Mcallister et al., *Chem. Mater.* 19 (2007) 4396.
- [10] Q. Yu, J. Lian, S. Siriponglert, H. Li, Y.P. Chen, S.S. Pei, *Appl. Phys. Lett.* 93 (2008) 113103.
- [11] J. Hass, W.A. de Heer, E.H. Conrad, *J. Phys.: Condens. Matter* 20 (2008) 323202.
- [12] M. Okano, R. Matsunaga, K. Matsuda, S. Masubuchi, T. Machida, Y. Kanemitsu, *Appl. Phys. Lett.* 99 (2011) 151916.
- [13] L.G. Booshehri et al., *Phys. Rev. B* 85 (2012) 205407.
- [14] S. Bae et al., *Nature Nanotechnol.* 5 (2010) 574.
- [15] T. Ohta, T.E. Beechem, J.T. Robinson, G.L. Kellogg, *Phys. Rev. B* 85 (2012) 075415.
- [16] J. Zabel, R.R. Nair, A. Ott, T. Georgiou, A.K. Geim, K.S. Novoselov, C. Casiraghi, *Nano Lett.* 12 (2012) 617.
- [17] Y. Hao et al., *Small* 6 (2010) 195.
- [18] K.H. Michel, B. Verberck, *Phys. Rev. B* 85 (2012) 094303.
- [19] J.W. Jiang, H. Tang, B.S. Wang, Z.B. Su, *Phys. Rev. B* 77 (2008) 235421.
- [20] S. Reich, S. Thomsen, *Philos. Trans. R. Soc. London, A* 362 (2004) 2271.
- [21] S.K. Saha, U.V. Waghmare, H.R. Krishnamurthy, A.K. Sood, *Phys. Rev. B* 78 (2008) 165421.
- [22] A.M. Popov, I.V. Lebedeva, A.A. Knizhnik, Y.E. Lozovik, B.V. Potapkin, *Chem. Phys. Lett.* 536 (2012) 82.
- [23] K. Sinha, J. Menéndez, *Phys. Rev. B* 41 (1990) 10845.
- [24] M. Hanfland, H. Beister, K. Syassen, *Phys. Rev. B* 39 (1989) 12598.
- [25] P.H. Tan et al., *Nat. Mater.* 11 (2012) 294.
- [26] A.H.R. Palser, *Phys. Chem. Chem. Phys.* 1 (1999) 4459.
- [27] D. Graf, F. Molitor, K. Ensslin, C. Stampfer, A. Jungen, C. Hierold, L. Wirtz, *Nano Lett.* 7 (2007) 238.
- [28] A.C. Ferrari et al., *Phys. Rev. Lett.* 97 (2006) 187401.
- [29] R.W. Havener, H. Zhuang, L. Brown, R.G. Henning, J. Park, *Nano Lett.* 12 (2012) 3162.
- [30] K. Kim et al., *Phys. Rev. Lett.* 108 (2012) 246103.